Available online at www.sciencedirect.com
SCIENCE DIRECT®
Earth and Planetary Science Letters 238 (2005) 342–350
EPSL
www.elsevier.com/locate/epsl

Testing a potential mantle geohygrometer; the effect of dissolved water on the intracrystalline partitioning of Al in orthopyroxene

S.C. Kohn [a,*], B.M. Roome [a], M.E. Smith [b], A.P. Howes [b]

[a] *Department of Earth Sciences, University of Bristol, Queens Rd., Bristol, BS8 1RJ, U.K.*
[b] *Department of Physics, University of Warwick, Coventry, CV4 7AL, U.K.*

Received 24 March 2005; received in revised form 12 August 2005; accepted 17 August 2005
Available online 21 September 2005
Editor: S. King

Abstract

The presence of water in the Earth's mantle has wide ranging implications and a detailed picture of the spatial and temporal distribution of water in the mantle is needed to be able to understand fundamental global-scale processes. However the interpretation of measured water concentrations in nominally anhydrous minerals (NAMs) from xenoliths or magmatic phenocrysts is complicated by fast diffusion of H and hence the probability of hydration or dehydration during ascent. Rauch and Keppler [1]M. Rauch, H. Keppler, Water solubility in orthopyroxene, Contrib. Mineral. Petrol. 143 (2002) 525–536 have proposed that the partitioning of Al between octahedral and tetrahedral sites in orthopyroxene has the potential to be used as a more reliable mantle geohygrometer than direct measurements of water concentrations in xenolith minerals. In the present study, we have tested the theoretical basis for this geohygrometer by experimentally producing aluminous orthopyroxene samples and measuring the intracrystalline partitioning of Al using very high-field ^{27}Al magic angle spinning nuclear magnetic resonance. In both dry and hydrous orthopyroxene, aluminium is shown to be incorporated by a Tschermak's substitution (one tetrahedral and one octahedral Al), thus the incorporation mechanism of Al in orthopyroxene is not a valid basis for a geohygrometer. However, the effect of OH on the local environment of Al has been observed, and quantification of all the different types of Al in the hydrous samples suggests that OH is incorporated by protonation of O21 and O22 sites. The results suggest that NMR studies on nuclei other than ^{1}H offer new possibilities for studying the interaction of water with mantle minerals.

Keywords: Water; Mantle; Orthopyroxene; Geohygrometer; NMR; ^{27}Al

1. Introduction

In recent years it has become widely acknowledged that water can play a crucial role in modifying the physical properties and behaviour of the Earth's mantle [2–8]. In particular the realisation that significant concentrations of water can be dissolved in nominally anhydrous minerals (NAMs) such as olivine, pyroxene and garnet has led to numerous measurements of water concentrations in natural mantle materials (e.g., [3,9,10]) and experimental studies of the solubility limits of water in NAMs (e.g., [11–14]). Diffusion studies have shown that H is very mobile in NAMs [3], therefore measurements of the water concentrations of minerals in xenoliths or magmatic phenocrysts are difficult to interpret, because of the potential for hydration or dehydration during ascent. These problems could be avoided if a suitable proxy structural or chem-

* Corresponding author. Tel.: +44 117 331 5002; fax: +44 117 925 3385.

0012-821X/$ - see front matter © 2005 Elsevier B.V. All rights reserved.
doi:10.1016/j.epsl.2005.08.011

ical signature for dissolved water concentration could be found; if this proxy had sufficiently slow re-equilibration kinetics it could be used as a geohygrometer to determine the original water concentration of xenoliths or phenocrysts.

One nominally anhydrous phase which has now been studied a number of times by different groups is orthopyroxene [1,15–18]. These studies have shown that the water solubility depends on pressure, temperature, the concentration of additional components, such as Al, Cr and V and possibly the silica activity. However, in detail, there are disagreements between the different studies concerning the quantification of water solubility, the mechanisms of water dissolution and the quantitative effects of the presence of additional chemical components. Some of the disagreements can be attributed to the methods used to quantify infrared spectra since different groups use different extinction coefficients and background subtractions. Unreported differences in chemical environments may also play a role.

One crucially important factor determining the solubility of water in natural orthopyroxenes is likely to be the concentration of aluminium. Mantle orthopyroxene contains aluminium and other trivalent cations, therefore coupled substitutions such as $Al^{3+}+H^{+}$ substituting for $2Mg^{2+}$ are to be expected and experimental studies so far have shown a strong correlation between Al and OH concentrations in Al-doped enstatite [1,15,16]. The magnitude of the effect is not clear however, as the effect of Al on the solubility of H reported by Rauch and Keppler [1] is several times larger than in the other studies. The experimental pressures and temperatures in all three studies are quite similar, so the reason for this discrepancy is puzzling. Rauch and Keppler [1] suggested that the coupled substitution could be expressed by the equilibrium

$$MgAl^{[6]}Al^{[4]}SiO_6 + H_2O + 2Mg_2SiO_4 \Rightarrow 2Mg_2Al^{[4]}HSiO_6 + MgSiO_3 \quad (1)$$

where $MgAl^{[6]}Al^{[4]}SiO_6$ is an orthopyroxene component with Al in Tschermak substitution and $Mg_2Al^{[4]}HSiO_6$ is an orthopyroxene component with tetrahedral Al only, charge balanced by H. They proposed that the intracrystalline partitioning of Al between octahedral and tetrahedral sites could therefore, in principle at least, be used as a geohygrometer for orthopyroxene, even when water is lost from a xenolithic or phenocrystic orthopyroxene during ascent and depressurisation.

However there are alternative possibilities for H and Al incorporation, such as the reaction

$$MgAl^{[6]}Al^{[4]}SiO_6 + H_2O + 7MgSiO_3 \Rightarrow 2HAl^{[6]}Si_2O_6 + 4Mg_2SiO_4 \quad (2)$$

suggested by [15], where $MgAl^{[6]}Al^{[4]}SiO_6$ is again an orthopyroxene component with Al in Tschermak substitution and $HAl^{[6]}Si_2O_6$ is an orthopyroxene component with octahedral Al only, charge balanced by H. Finally the H could be incorporated without any change in the ratio of octahedral : tetrahedral aluminium, via reactions such as

$$MgAl^{[6]}Al^{[4]}SiO_6 + H_2O \Rightarrow H_2Al^{[6]}Al^{[4]}SiO_6 + MgO \quad (3)$$

$$MgAl^{[6]}Al^{[4]}SiO_6 + 2H_2O \Rightarrow MgAl^{[6]}Al^{[4]}H_4O_6 + SiO_2 \quad (4)$$

These reactions are analogous to the protonation of Mg or Si vacancies in Al-free orthopyroxene, but could potentially be enhanced by the presence of Al, and therefore explain the increase in water solubility as a function of increasing Al concentration.

The aim of the present study is therefore to synthesise both dry and hydrous aluminous enstatite and to study the intracrystalline Al partitioning using ^{27}Al magic angle spinning nuclear magnetic resonance (MAS NMR). ^{27}Al MAS NMR has been shown to be an excellent atomic scale probe of the environment of aluminium, readily distinguishing AlO_4, AlO_5 and AlO_6 local environments [19–21]. The different local coordinations can be readily identified through their different chemical shifts. Nuclei like aluminium, which have a nuclear spin $>1/2$, also experience a nuclear electric quadrupole interaction arising from the interaction between the electric quadrupole moment of the nucleus (eQ) and the electric field gradient at the nucleus (eq). This interaction is usually characterised by the quadrupole coupling constant ($\chi_Q = e^2Qq/h$) and asymmetry parameter (η) [19,22]. The results will be used to test the theoretical basis for an Al-based geohygrometer for aluminous orthopyroxene.

2. Experimental methods

2.1. Sample synthesis

The samples were prepared from glass starting materials. The glass was made by finely grinding mixtures of MgO, SiO_2 and Al_2O_3, melting these mixtures at

1700 °C for one hour, then quenching the melts rapidly into water. The resulting glass was then finely ground before being used as the starting material in synthesis of crystalline orthopyroxenes. All compositions were made with a slight excess of MgO over the stoichiometric pyroxene composition to ensure forsterite buffering. Orthopyroxene samples were then synthesised by loading the powdered glass starting material, either with or without water into 6 mm Pt capsules, welding them shut, then annealing at 2 GPa and 1200 °C using a piston cylinder apparatus with a tapered graphite furnace and a talc/pyrex pressure cell, for times up to 66 h (Table 1). A piston-in technique was used and no pressure correction was applied, therefore the actual pressure could be somewhat lower than the nominal pressure. In the case of the two wet samples described here, water escaped when the capsule was pierced after the run, demonstrating that the orthopyroxene in these runs must have been water saturated. Additionally some dry samples were synthesised at 1 bar pressure.

2.2. Sample characterisation

The composition and mineralogy of the samples were checked using electron probe microanalysis (EPMA) and X-ray diffraction (XRD). All samples except BR14 contain mostly aluminous orthopyroxene with a few percent forsterite. BR14 contained no other phases. The average aluminium concentrations in the orthopyroxene are generally quite close to those expected (Table 1). However the Al concentrations of the wet samples are lower than those of the dry samples, possibly because of dissolution of Al in the fluid during synthesis. It should also be noted that some samples are somewhat heterogeneous in terms of Al concentration.

No attempt was made to measure the water concentrations of the samples because the crystals formed in the syntheses were too small for analysis using single crystal FTIR. However, the water concentration of the wet samples can be estimated from previous work from other groups and recent work performed in Bristol [18]. As mentioned earlier, the data of [1] suggest much higher water concentrations than other studies; extrapolation of their data would predict water concentrations as high as 10,000 wt ppm H_2O, which seems unrealistic. Data from [16] imply solubilities of 1300 wt ppm H_2O for orthopyroxene with 5.03 wt.% Al_2O_3, and 800 wt ppm H_2O for orthopyroxene with 2.83 wt.% Al_2O_3 under similar pressure and temperature conditions. These values are more comparable with data from our laboratory (e.g., [18]) and will be used in calculations in this paper. In both cases, these figures give an estimate of the H : Al ratio of 1 : 7, i.e., for every 7 aluminium atoms incorporated in the structure, 1 additional hydroxyl can be incorporated under these pressure and temperature conditions. BR14 is unequivocally anhydrous as it was synthesised at 1 bar pressure. It is not impossible that BR11 and BR12 contain some water despite being nominally anhydrous, because of diffusion of H into the capsule during the run, however this is not considered to be a significant problem because of the similarity in the ^{27}Al spectra spectra for BR14, BR11 and BR12 (see below), and the strong contrast with the water saturated samples.

Table 1
Synthesis conditions and characterisation of samples

Sample name	Synthesis conditions	Nominal bulk wt.% Al_2O_3	Actual wt.% Al_2O_3 in orthopyroxene[a]
BR11	2GPa 1200 °C dry	4	4.44 ± 1.28
BR4	2GPa 1200 °C wet	4	2.83 ± 0.32
BR14	0.1 MPa 1200 °C dry	6	5.66 ± 0.19
BR12	2GPa 1200 °C dry	6	5.95 ± 0.33
BR13	2GPa 1200 °C wet	6	5.03 ± 0.36

[a] Error given is one standard deviation. The error is due to a combination of real heterogeneity in the samples and analytical error.

2.3. ^{29}Si nuclear magnetic resonance

^{29}Si MAS NMR was used as an additional method for checking the phases present in the samples. All the spectra (Fig. 1) were obtained using Chemagnetics CMX Infinity spectrometers and the spectra were referenced to TMS at 0 ppm. The spectra of the Al-bearing orthopyroxene samples were run at 8.45 T and a frequency of 71.54 MHz using a 1.2 μs pulse corresponding to tip angle of ~30° and recycle delay of 30 s; a Chemagnetics 6 mm probe was used with spinning at 4 kHz. In addition a previously unpublished spectrum for pure Al-free synthetic enstatite will be used here to compare with the Al bearing samples. This spectrum was obtained at 7.05 T and a frequency of 59.66 MHz using a 1.5 μs pulse and a recycle delay of 60 s. A 4 mm probe was used, with spinning at 5 kHz.

2.4. ^{27}Al nuclear magnetic resonance

The concentrations of tetrahedral and octahedral Al in the samples were determined using ^{27}Al MAS NMR. Initial measurements at a field of 9.4 T, using a Bruker DMX 400 spectrometer at Bristol University, suggested that the tetrahedral site is very distorted with a very large quadrupole coupling constant (χ_Q). This magnetic field (B_o) was therefore not adequate to measure the Al

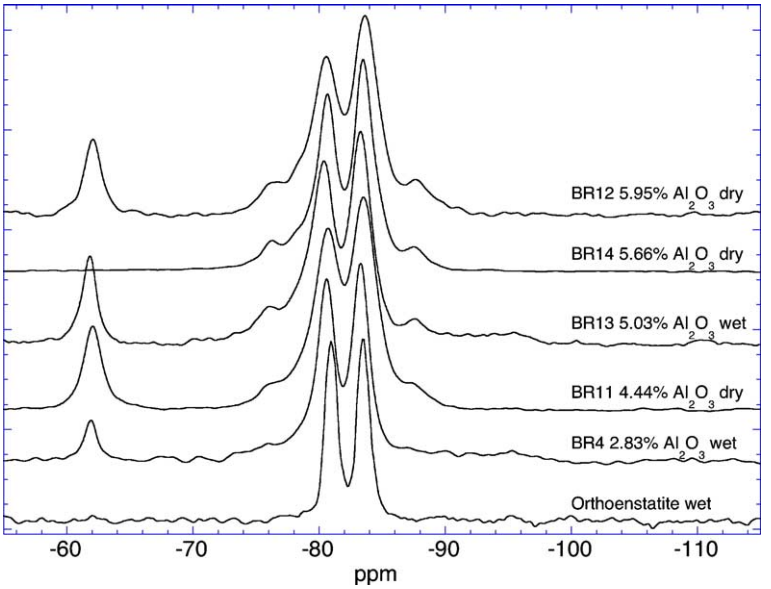

Fig. 1. ^{29}Si MAS NMR spectra of all samples, stacked in order of increasing Al_2O_3 concentration, together with a spectrum for Al-free orthoenstatite.

partitioning between tetrahedral and octahedral sites in the orthopyroxene. Additional measurements at much higher magnetic fields of 14.1 T (Warwick University), 16.4 T and 18.8 T (Rutherford Appleton Laboratory) were therefore performed at ^{27}Al resonance frequencies of 156.37, 182.43, and 208.37 MHz, respectively. All these experiments were carried out on Varian CMX Infinity spectrometers using T3 MAS probes of either 2.5 or 4 mm diameter. One pulse experiments were performed using small tip angle pulses ($<\pi/12$) and recycle delays of 5 s, thereby ensuring that the spectra obtained could be used quantitatively. Spectra were referenced against the AlO_6 resonance of $Y_3Al_5O_{12}$ at 0.7 ppm, a secondary reference such that 0 ppm corresponds to $[Al(H_2O)_6]^{3+}$.

The 18.8 T MAS NMR spectra shown in Figs. 2 and 3 were acquired using a 4 mm diameter rotor, which has the advantages of a reasonable sample volume, and

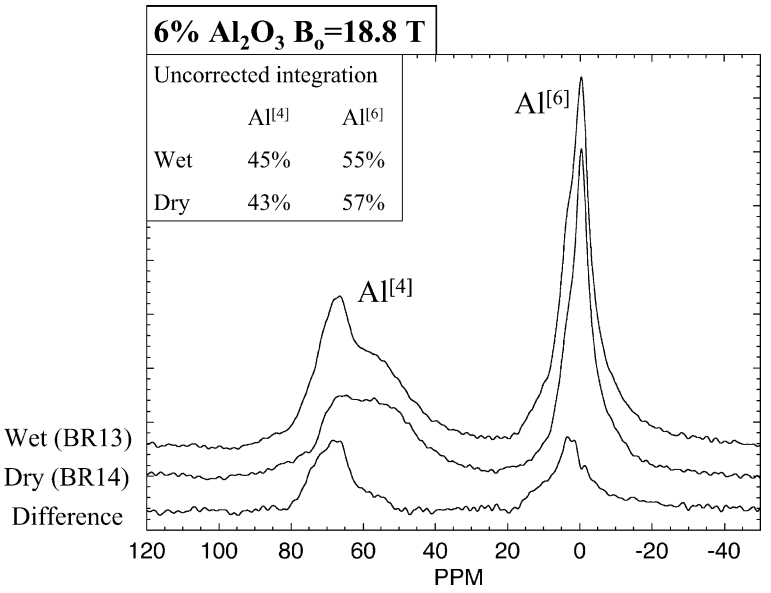

Fig. 2. ^{27}Al NMR spectra of samples containing 6 wt.% Al_2O_3 (nominal), obtained at a magnetic field of 18.8 T. Upper spectrum is BR13, middle is BR14 and lower is the subtraction of BR14 from BR13.

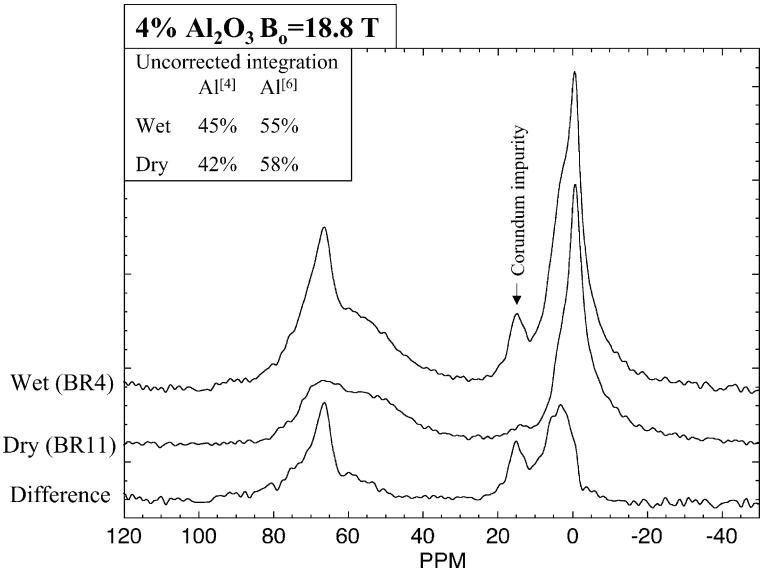

Fig. 3. ^{27}Al NMR spectra of samples containing 4 wt.% Al_2O_3 (nominal), obtained at a magnetic field of 18.8 T. Upper spectrum is BR4, middle is BR11 and lower is the subtraction of BR11 from BR4.

hence good signal to noise ratio, and a negligible ^{27}Al signal from the ZrO_2 rotor, but the spinning speed was limited to 20 kHz. Some additional spectra were also collected using a 2.5 mm rotor; this has the advantage of higher available spinning speeds (in excess of 25 kHz), but with a significant reduction in signal to noise ratio, and most importantly a significant ^{27}Al signal from the rotor, which has to be subtracted after acquisition.

3. Results

^{29}Si MAS NMR spectra are shown in Fig. 1. The spectrum of pure orthoenstatite consists of two narrow peaks at −81.0 and −83.5 ppm, corresponding to resonances from silicon T1 and T2 sites. Additional peaks at −76.6, −78.4 and −87.6 appear in Al-bearing samples and all the peaks broaden with increasing Al_2O_3 concentration. The exact assignment of the additional peaks is complex, because of the competing effects of substituting Al for Mg in an octahedral site and Al for Si in a tetrahedral site and the fact that even in Al-free enstatite there are two distinct sites. A very similar effect was observed in a ^{29}Si study of pyroxenes in the Di-CaTs system [23], and by analogy with the assignments given in that paper, the peak at −76.6 ppm corresponds to silicons shifted from −81.0 ppm because of substitution of one Al into the adjacent tetrahedral site, the peak at −87.6 ppm is due to a shifting of the −83.5 ppm peak by substitution of Al into an adjacent octahedral site. The assignment of the −78.4 ppm shoulder is slightly less certain, but it is probably due to a shift of the −83.5 ppm peaks because of substitution of one Al into the adjacent tetrahedral site. The only other features of note are peaks for forsterite at −62 ppm [24] in all spectra apart from that for BR14, and a very small feature at about −95 ppm in the three samples which were prepared in the presence of an aqueous phase. We assign this small feature to a small quantity of an Al-free sheet silicate phase, such as sepiolite, which probably precipitated on the quench. The deduction that the phase which gives this peak is Al-free is important and is supported by two strands of evidence: i) The peak is present in the Al-free orthopyroxene sample; and ii) there is no peak in the ^{27}Al NMR spectra which could result from the presence of an aluminosilicate sheet mineral (see below).

^{27}Al MAS NMR spectra for wet and dry orthopyroxene samples with nominally 6 wt.% dissolved Al_2O_3, obtained at 18.8 T are shown in Fig. 2. The dry sample consists of a broad peak around 60 ppm which is due to tetrahedral Al and a narrower peak at 0 ppm which is due to octahedral Al. The spectrum for the sample made under wet conditions is similar, but has an extra narrower component which is visible in the tetrahedral region of the spectrum. Both spectra were integrated to give the ratio of tetrahedral to octahedral Al and the results of the integrations are given in Table 2 as 'uncorrected $Al^{[4]}:Al^{[6]}$'. The true $Al^{[4]}:Al^{[6]}$ is obtained by a small correction to these values (see below). The bottom spectrum in the figure is a subtraction of the dry spectrum from the wet spectrum. It shows that there is also a new feature in the octahedral

Table 2
Summary of integrations of 18.8 T ^{27}Al NMR data

Sample name	Actual wt.% Al_2O_3 in orthopyroxene	Estimated ppm H_2O	Estimated H:Al ratio	Uncorrected $Al^{[4]}:Al^{[6]}$ (±2:±2)	Corrected[a] $Al^{[4]}:Al^{[6]}$	% $Al^{[4]}$ in modified site[b]	% $Al^{[6]}$ in modified site
BR11	4.44±1.28	0	0	42:58	46:54	–	–
BR4	2.83±0.32	800	1:6.3	45:55	48:52	35	35
BR14	5.66±0.19	0	0	43:57	47:53	–	–
BR12	5.95±0.33	0	0	n/m[c]	n/m[c]	–	–
BR13	5.03±0.36	1300	1:6.9	45:55	48:52	29	26

[a] The correction of the $Al^{[4]}:Al^{[6]}$ was performed by multiplying the observed intensity of $Al^{[4]}$ by 100/85 for dry samples, to allow for the fact that only 85% of the intensity of $Al^{[4]}$ is observed in the centreband. For wet samples a factor of 100/90 was used, because approximately 30% of the Al in the wet samples is in the 'H-modified' environment. This H-modified Al does not have a large χ_Q and its signal therefore does not require correction factor to be applied. The absolute errors on the tetrahedral site concentrations calculated from the uncertainties in integration, χ_Q and η are +7/−3, but sample to sample error is only around ±2.
[b] Corrected by assuming 100% of modified site, and 85% of unmodified site is observed.
[c] Sample BR12 was not measured at 18.8 T, but spectra were obtained at the lower fields, and were found to be very similar to those for BR14.

region which is not visible by inspection of the individual spectra. These extra features are interpreted as Al environments modified by the presence of H in the orthopyroxene structure. The concentrations of these modified Al species were also obtained by integration and are given in Table 2.

Very similar spectra are seen for the samples with nominally 4 wt.% dissolved Al_2O_3, shown in Fig. 3. The main difference is that the wet sample contains a small amount of corundum as an impurity. This was subtracted in all quantifications of the spectra. The results of integrating the spectra are also given in Table 2.

As mentioned previously, a small correction has to be applied to quantification of ^{27}Al NMR spectra because of differences in the quadrupole coupling constants (χ_Q) between sites. Fig. 4 shows the ^{27}Al MAS NMR spectrum of BR11 at three different magnetic fields. A dashed line is included to illustrate the loss of resolution at the lower magnetic fields. The residual line width (in ppm) of MAS spectra where second-order quadrupole effects dominate varies as B_o^{-2} [19,22]. It can be seen that both $Al^{[4]}$ and $Al^{[6]}$ spectral regions are broader at the lower magnetic fields, but the effect is especially marked for the $Al^{[4]}$ region, indicating that it is experiencing a much larger χ_Q. These data are extremely useful because the χ_Q of the two different sites can be estimated by plotting the centre of gravity of each peak (in ppm) as a function of the inverse square of the Larmor frequency [22,25,26]. The centre of gravity of both peaks at 18.8 and 16.4 T and the $Al^{[6]}$ peak at 14.1 T can be measured with some confidence. For the $Al^{[4]}$ peak at 14.1 T a reasonable estimate can be made by taking the higher field line shapes and extrap-

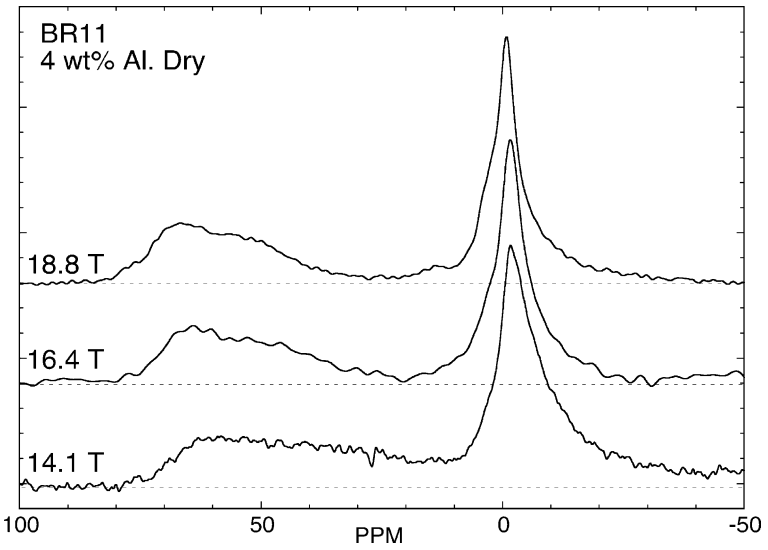

Fig. 4. ^{27}Al NMR spectra of BR11 at three different magnetic fields. Note the increasing line widths, especially of the tetrahedral site, at lower fields.

olating them to the lower field using the well known field dependence of such line shapes. This procedure produces estimates of χ_Q for the tetrahedral and octahedral sites of 13 ± 2 and 3 ± 1 MHz, respectively. It is very clear that the quadrupole interaction of the tetrahedral sites of the orthopyroxene is much larger than that of the octahedral sites. There are not enough data to accurately estimate χ_Q for the H-modified tetrahedral or octahedral sites, but their line shapes, and in particular their relative residual MAS line widths suggest that they probably experience χ_Q in the range 3–5 MHz. It is unlikely that any sheet aluminosilicates precipitated from the fluid contribute to the signal for the H-modified sites, as they would have $\chi_Q < 3$MHz for both tetrahedral and octahedral sites [20].

In an MAS NMR spectrum the intensity will be spread between the centreband and the spinning side bands. For quadrupole nuclei there is the central $+1/2 \Leftrightarrow -1/2$ transition that dominates the spectra, and satellite transitions which are usually spread over ~MHz which can effectively be neglected in most cases. In an ideal case the spinning speeds employed would be fast enough that all the $+1/2 \Leftrightarrow -1/2$ transition intensity is contained within the centrebands for all the different sites. However in the experiments here the spinning speeds are insufficient to eliminate equally spinning side bands of the $+1/2 \Leftrightarrow -1/2$ transition between the different sites. The ^{27}Al MAS NMR spectra obtained here with a spinning speed of 25 kHz provide enough resolution to show that the tetrahedral site has substantial $+1/2 \Leftrightarrow -1/2$ transition spinning side bands, whereas the octahedral site does not. This reinforces the interpretation that signal loss is occurring from the centreband of the $Al^{[4]}$ peak compared to $Al^{[6]}$, and that the centreband intensity needs to be corrected to obtain the actual aluminium distribution between the different coordinations.

The dependence of the fraction of the ^{27}Al signal observed in the centreband is a known function of the spinning speed (ν_r), the quadrupole frequency ($\nu_Q = 3e^2Qq/20h$), and the Larmor frequency (ν_0) [22,27].These parameters are all now known, so the fraction of Al signal observed in the centreband can be calculated graphically (Fig. 5). For $Al^{[4]}$, $(\nu_Q)^2/(\nu_0\nu_r)$ is 1.13, so 80–90% of the Al central transition signal is observed in the centreband at 18.8 T (depending on the value of η, the asymmetry parameter, which is unknown). For $Al^{[6]}$, $(\nu_Q)^2/(\nu_0\nu_r)$ is 0.06, so 100% of the Al central transition signal is observed in the centreband at 18.8 T. For the H-modified sites essentially all the central transition signal is also observed. The correction factors calculated above were applied to the uncorrected data and the corrected values of $Al^{[4]}$:$Al^{[6]}$ and the concentrations of H-modified $Al^{[4]}$ and $Al^{[6]}$ in the wet samples are given in Table 2.

The key observation is that there is no systematic difference in the $Al^{[4]}$:$Al^{[6]}$ ratio between wet and dry samples. The ratio is also close (within error) to the expected value of 50:50 for a charge balanced Tschermak's substitution. The fact that the concentration of

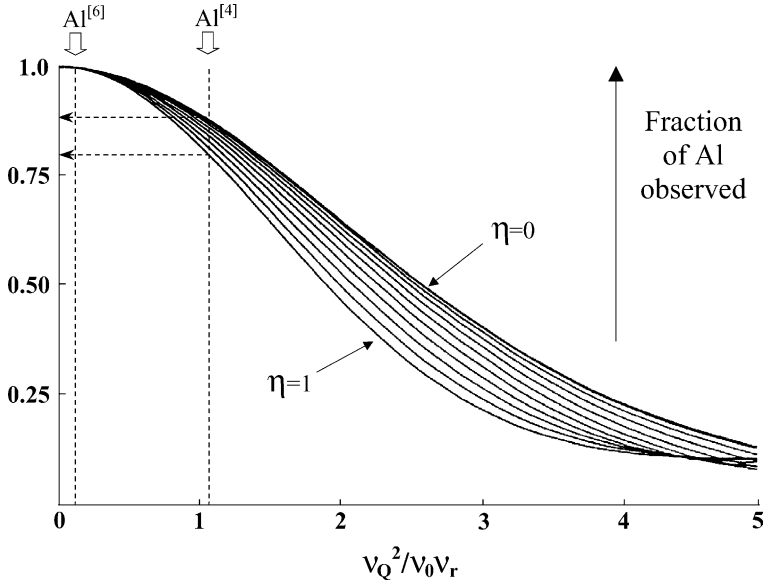

Fig. 5. Plot of fraction of Al observed in the MAS centreband as a function of $(\nu_Q)^2/(\nu_0\nu_r)$ [22,27], together with data for the tetrahedral and octahedral sites in BR11. ν_r is the spinning speed, ν_Q is the quadrupole frequency, ν_0 is the Larmor frequency and η is the asymmetry parameter.

$Al^{[4]}$ is slightly less than 50% in all cases probably reflects a small underestimate in χ_Q for the tetrahedral site. A value of $\chi_Q = 14$–15 MHz (within our estimated error) would give the expected 50:50 ratio. If our assumption of 800 ppm H_2O for BR4 and 1300 ppm H_2O for BR13 are correct, the expected $Al^{[4]}:Al^{[6]}$ ratio for H incorporation by reaction (1) is 58:42, significantly different from that which is observed. If the higher water solubilities reported by [1] are correct, the predicted $Al^{[4]}:Al^{[6]}$ ratio would be even higher, and further from the observed ratio.

One final scenario must be considered. If there are new Al environments in wet orthopyroxene which have extremely high values of χ_Q, such that $(\nu_Q)^2/(\nu_0\nu_r)$ is in excess of 5, it is possible that they could be overlooked completely. However, it is relatively easy to test this possibility by making measurements on weighed samples, and comparing the integrated and mass-scaled signals with dry orthopyroxene and standard samples. Such measurements were made for BR14 and BR13 using α-alumina and γ-alumina as standards, spinning at 25 kHz using a 2.5 mm rotor at 18.8 T. There are substantial errors in quantifying the data, depending on the method used for processing the data, but the average of all methods gives 5.08 ± 0.2 wt.% Al_2O_3 for BR13 and 4.97 ± 0.2 wt.% Al_2O_3 for BR14. Within error these numbers are in agreement with our independent estimates based on EPMA, and the fraction of Al observed (Fig. 5), which come to 4.78 ± 0.3 wt.% Al_2O_3 for BR13 and 5.24 ± 0.2 wt.% Al_2O_3 for BR14.

4. Discussion

The data described above show conclusively that under forsterite buffered conditions, water dissolution in aluminous enstatite does not occur exclusively via either reaction described by Eqs. (1) or (2). In both dry and hydrous orthopyroxene, aluminium is incorporated by a Tschermak's substitution, thus the incorporation mechanism of Al in orthopyroxene is not a valid basis for a geohygrometer. The remaining questions are: — why is there a correlation between water solubility and Al concentration? and what is the site of water incorporation? One interesting aspect of our data is that the amount of Al in the H-modified tetrahedral and octahedral sites is 35 ± 4% for BR4 and 27 ± 4% for BR13, whereas our best estimate of H:Al in the samples suggests that 15.8% of the Al in BR4 and 14.5% of the Al in BR13 would be modified if one H was localised on each Al. If each H incorporated modifies the environment of one tetrahedral and one octahedral site, the prediction would of course be 31.6% and 29%, respectively, in excellent agreement with the observed NMR data. A good model for H incorporation would therefore involve protonation of oxygens such as O21 and O22 which bridge between tetrahedral and octahedral M1 sites in the structure of orthopyroxene (M1 is almost certainly the site occupied by octahedral Al in orthopyroxene as it is smaller than M2). This model is consistent with the orientation of OH dipoles observed in aluminous orthopyroxene [15,16,18,28], if the OH is oriented approximately along the O21–O11 and O22–O12 directions. Previous work (e.g., [15]) has attempted to use the O–O distances in unprotonated NAMs to determine the sites of OH incorporation by applying empirical correlations between O–H stretching frequency and O–O distance [29]. This is a reasonable approach, but should be used with some caution because recent work [14] has shown that it fails for olivine, presumably because of modification of local environments by cation vacancies and the presence of H.

5. Conclusions

Several important conclusions can be drawn from the data reported here. The key observation is that the $Al^{[4]}:Al^{[6]}$ ratio in aluminous enstatite is the same in both wet and dry samples, and within error of the expected value of 1:1. This clearly indicates that $Mg_2Al^{[4]}HSiO_6$ is not the dominant incorporation mechanism and that measurements of the intracrystalline partitioning of Al in orthopyroxene is not a viable method for determining the original H_2O concentration in xenoliths. New $Al^{[4]}$ and $Al^{[6]}$ sites are observed in the wet samples, and their abundance suggests that every H incorporated into the orthopyroxene modifies the local environment of approximately two Al sites (assuming that our estimates of the water concentrations of the samples are correct). The most likely explanation is that O21 and O22 are the sites for protonation in aluminous orthopyroxene.

Acknowledgments

The authors would like to thank NERC for financial support, and EPSRC and the University of Warwick for partial funding of the NMR equipment. Comments by two anonymous reviewers improved the manuscript.

References

[1] M. Rauch, H. Keppler, Water solubility in orthopyroxene, Contrib. Mineral. Petrol. 143 (2002) 525–536.
[2] P.D. Asimow, C.H. Langmuir, The importance of water to oceanic mantle melting regimes, Nature 421 (2003) 815–820.

[3] J. Ingrin, H. Skogby, Hydrogen in nominally anhydrous upper-mantle minerals: concentration levels and implications, Eur. J. Mineral. 12 (2000) 543–570.
[4] D. Bercovici, S. Karato, Whole-mantle convection and the transition-zone water filter, Nature 425 (2003) 39–44.
[5] S. Karato, H. Jung, Water, partial melting and the origin of the seismic low velocity and high attenuation zone in the upper mantle, Earth Planet. Sci. Lett. 157 (1998) 193–207.
[6] G. Hirth, D.L. Kohlstedt, Water in the oceanic upper mantle: implications for rheology, melt extraction and the evolution of the lithosphere, Earth Planet. Sci. Lett. 144 (1996) 93–108.
[7] G. Richard, M. Monnereau, J. Ingrin, Is the transition zone an empty water reservoir? Inferences from numerical model of mantle dynamics, Earth Planet. Sci. Lett. 205 (2002) 37–51.
[8] J.E. Dixon, T.H. Dixon, D.R. Bell, R. Malservisi, Lateral variation in upper mantle viscosity: role of water, Earth Planet. Sci. Lett. 222 (2004) 451–467.
[9] D.R. Bell, G.R. Rossman, Water in Earth's mantle — the role of nominally anhydrous minerals, Science 255 (1992) 1391–1397.
[10] D.R. Bell, G.R. Rossman, R.O. Moore, Abundance and partitioning of OH in a high-pressure magmatic system: megacrysts from the Monastery Kimberlite, South Africa, J. Petrol. 45 (2004) 1539–1564.
[11] A.C. Withers, B.J. Wood, M.R. Carroll, The OH content of pyrope at high pressure, Chem. Geol. 147 (1998) 161–171.
[12] D.L. Kohlstedt, H. Keppler, D.C. Rubie, Solubility of water in the alpha, beta and gamma phases of $(Mg, Fe)_2SiO_4$, Contrib. Mineral. Petrol. 123 (1996) 345–357.
[13] S.C. Kohn, Solubility of H_2O in nominally anhydrous mantle minerals using ^1H MAS NMR, Am. Mineral. 81 (1996) 1523–1526.
[14] C. Lemaire, S.C. Kohn, R.A. Brooker, The effect of silica activity on the incorporation mechanisms of water in synthetic forsterite: a polarised infrared spectroscopic study, Contrib. Mineral. Petrol. 147 (2004) 48–57.
[15] R. Stalder, H. Skogby, Hydrogen incorporation in enstatite, Eur. J. Mineral. 14 (2002) 1139–1144.
[16] R. Stalder, Influence of Fe, Cr and Al on hydrogen incorporation in orthopyroxene, Eur. J. Mineral. 16 (2004) 703–711.
[17] K. Mierdel, H. Keppler, The temperature dependence of water solubility in enstatite, Contrib. Mineral. Petrol. 148 (2004) 305–311.
[18] K.J. Grant, S.C. Kohn, R.A. Brooker, Solubility and partitioning of water in synthetic forsterite and enstatite in the system MgO-SiO_2-$H_2O \pm Al_2O_3$, Contrib. Mineral. Petrol. (submitted for publication).
[19] K.J.D. MacKenzie, M.E. Smith, Multinuclear Solid State Nuclear Magnetic Resonance of Inorganic Materials, Pergamon Press, 2002.
[20] M.E. Smith, ^{27}Al NMR structure determination in solids, Appl. Magn. Reson. 4 (1993) 1–64.
[21] D. Freude, Quadrupolar nuclei in solid-state nuclear magnetic resonance, in: Meyers R.A., editor. Encyclopedia of Analytical Chemistry, Chichester: John Wiley and Sons, Ltd., 2000.
[22] M.E. Smith, E.R.H. van Eck, Recent advances in experimental solid state NMR methodology for half-integer spin quadrupolar nuclei, Prog. Nucl. Magn. Reson. Spectrosc. 34 (1999) 159–201.
[23] R.L. Flemming, W.W. Luth, ^{29}Si MAS NMR study of diopside-Ca-Tschermak clinopyroxenes: detecting both tetrahedral and octahedral Al substitutions, Am. Mineral. 87 (2002) 25–36.
[24] M. Magi, E. Lippmaa, A. Samoson, G. Engelhardt, A.-R. Grimmer, Solid-state high-resolution silicon-29 chemical shifts in silicates, J. Phys. Chem. 88 (1984) 1518–1522.
[25] S.C. Kohn, R. Dupree, M.E. Smith, A multinuclear magnetic resonance study of the structure of hydrous albite glasses, Geochim. Cosmochim. Acta 53 (1989) 2925–2935.
[26] S.C. Kohn, M.E. Smith, P.J. Dirken, E.R.H. van Eck, A.P.M. Kentgens, R. Dupree, Sodium environments in dry and hydrous albite glasses: improved ^{23}Na solid state NMR data and their implications for water dissolution mechanisms, Geochim. Cosmochim. Acta 62 (1998) 79–87.
[27] D. Massiot, C. Bessada, J.P. Coutures, F. Taulelle, A quantitative study of aluminum-27 MAS NMR in crystalline YAG, J. Magn. Res. 90 (1990) 231–242.
[28] A. Beran, J. Zemann, The pleochroism of a gem-quality enstatite in the region of the OH stretching frequency, with a stereochemical interpretation, TMPM, Tschermaks Mineral. Petrogr. Mitt. 35 (1986) 19–25.
[29] E. Libowitzky, Correlation of O–H stretching frequencies and O–H O hydrogen bond lengths in minerals, Mon. Chem. 130 (1999) 1047–1059.